

# Active Galactic Nuclei, Radio Jets and Acceleration of UHECRs

S. Massaglia<sup>a</sup>

<sup>a</sup>Dipartimento di Fisica Generale dell'Università,  
Via Pietro Giuria 1, 10125 Torino, Italy

We present the general properties of the Active Galactic Nuclei (AGNs) and discuss the origin and structure of jets that are associated to a fraction of these objects. We then we address the problems of particle acceleration at highly relativistic energies and set limits on the luminosity of AGN jets for being origin of UHECRs.

## 1. INTRODUCTION

Most of the galaxies of the Local Universe shine by effect of stellar and interstellar gas emissions, predominantly in the optical band. Typically, the emitted spectra are characterized by stellar absorption lines and emission lines by HII regions. These sources are called *Normal Galaxies*. A small fraction of galaxies, about 1%, do not follow this behavior. In fact, they show strong and broad emission lines, consistent with velocity dispersion of the emitting gas attaining several thousand of kilometers per second. Most remarkably, the non-thermal emission coming from a central nucleus, with size  $\sim 10^{-2}$  pc, dominates over the thermal one coming from stars and interstellar gas and extends well beyond the optical band, from radio to gamma rays (Fig. 1). These sources are called *Active Galaxies* and host *Active Galactic Nuclei* (AGNs) at their centers. AGNs are not all the same, on the contrary they can be extremely different in their properties. It resulted convenient to classify AGNs according to their radio power, in fact they can be separated into two distinct classes: Radio Quiet and Radio Loud AGNs. Typically, the luminosity in the GHz band of radio loud AGNs exceeds the radio quiet ones by about three orders of magnitudes. Observationally, Seyfert 1 show broad emission lines in the spectrum (Broad Line Region, BLR, with velocity dispersion  $\sigma \sim 10^4$  km s<sup>-1</sup>), while for Seyfert 2 the spectral lines are narrower (Narrow Line Region, NLR,  $\sigma \leq 10^3$  km s<sup>-1</sup>). Table 1 summarizes the objects belonging to the two

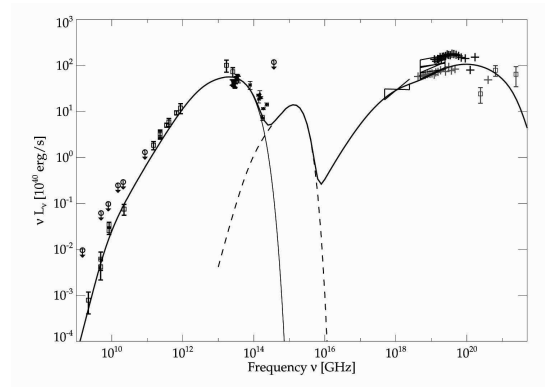


Figure 1. Spectral Energy Distribution of the Centaurus A core. The continuous line is a synchrotron plus Synchrotron Self-Compton (SSC) model [22].

classes.

This complex “zoology” has been interpreted by [27] within the so called Unified Model for AGNs. According to this picture (Fig. 2), radio quiet AGNs have no jets (or very weak ones) while the radio loud ones have jets; the angle between the line of sight and the plane of the obscuring torus determines the observed properties of AGNs. We will discuss the main properties of radio loud AGNs, in particular of the radio galaxies, since the presence of a jet may be crucial for accelerating cosmic ray at the highest energies.

Table 1

Radio quiet AGNs	Radio loud AGNs
Seyfert I galaxies (Sey 1) (BLR, $\sigma \sim 10^4 \text{ km s}^{-1}$ )	Radio galaxies
Seyfert II galaxies (Sey 2) (NLR, $\sigma \leq 10^3 \text{ km s}^{-1}$ )	Radio quasars
Radio quiet quasars (QSOs)	BL Lac Objects
	Optically Violent Variables (OVVs)

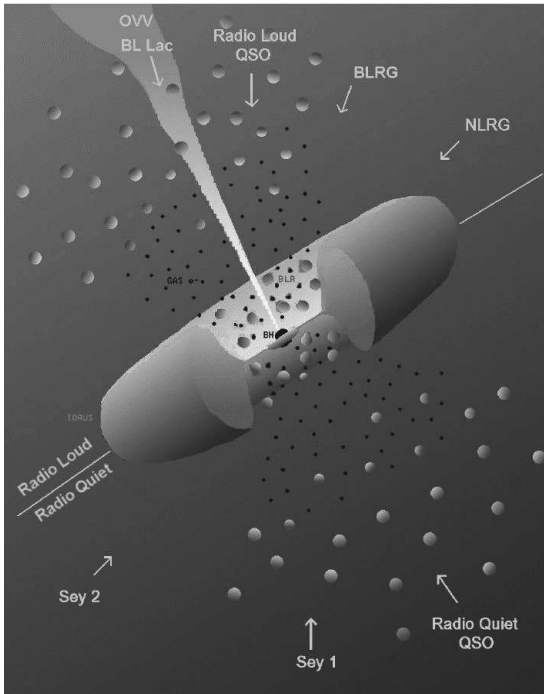


Figure 2. The unified AGN model

In Section 2 we review the main properties of radio galaxies and in Section 3 we will discuss the particle acceleration from AGN jets. The main outcomes are summarized in Section 4.

## 2. THE RADIO GALAXIES

Radio galaxies are seen in the radio band emitting power-law spectra, indicative of synchrotron emission with typical spectral index  $\alpha \sim 0.5$ . Moreover, jets and hot-spots of some bright

sources are seen in the optical and X-ray bands as well. The emission mechanism at these higher frequencies is again continuum and it may be synchrotron or Synchrotron-Self-Compton. Direct observations of radio galaxies give us: i) the radio luminosity  $\sim 10^{39} - 10^{44} \text{ ergs s}^{-1}$ ; ii) the size, from a few kiloparsec to some megaparsec; iii) the morphological brightness distribution, and iv) the polarization degree of the radio emission. We can then derive, by indirect means, the main physical parameters such as the life timescale,  $10^7 - 10^8 \text{ ys}$ , the mean magnetic field,  $10 - 10^3 \mu\text{G}$ , and the kinetic power,  $10^{42} - 10^{47} \text{ ergs s}^{-1}$ . The values of the jet main physical parameters, such as jet velocity, density and composition, are still under debate after many decades of investigations. The reason for these uncertainties in constraining the basic physical parameters is due to the very nature of the radiation emission which is typically non-thermal continuum, i.e. the absence of any lines in the radiation spectrum [17]. Therefore, the value of the magnetic field is derived by the minimum energy assumption, the jet kinetic power by the work done against the ambient to evacuate cavities for accommodating the radio lobes, the jet velocity by the radiative flux contrast of the approaching to receding jets and by proper motion observations, and the jet density by comparison between observed morphologies and the outcome of numerical simulations.

### 2.1. The Fanaroff-Riley Classification

Historically, the extragalactic radio sources have been classified into two categories [6] based upon their radio morphology: a first class of objects, preferentially found in rich clusters and hosted by weak-lined galaxies, shows jet-dominated emission and two-sided jets and was

named FR I; a second one, found isolated or in poor groups and hosted by strong emission-line galaxies, presents lobe-dominated emission and one-sided jets and was called FR II (or “classical doubles”). Besides morphology, FR I and FR II radio sources were discriminated in power as well: objects below  $\sim 2 \times 10^{25} h_{100}^2 \text{ W Hz}^{-1} \text{ str}^{-1}$  were typically referred as FR I sources. A perhaps more illuminating criterion has been found by [14] who plotted the radio luminosity at 1.4 GHz against the optical absolute magnitude of the host galaxy: they found the bordering line of FR I to FR II regions correlating as  $L_R \propto L_{opt}^{1.7}$  (Fig. 3), i.e. in a luminous galaxy more radio power is required to form a FR II radio sources. This correlation is important since it can be interpreted as an indication that the environment may play a crucial role in determining the source structure. The above argument yields the basic question of the origin of FR I/FR II dichotomy, whether intrinsic or ambient driven [17]. We note as well that there are no sources below a luminosity of  $10^{23} \text{ W Hz}^{-1}$  (at 1.4 GHz).

### 3. COSMIC RAY ACCELERATION

The problem of the sites of cosmic ray acceleration, after many decades of experimental and theoretical investigations, is not yet solved. Concerning the cosmic rays in the highest-energy region, above  $E = 3 \times 10^{18} \text{ eV}$ , there is a common, even though not unanimous, agreement about an extragalactic origin. Several mechanisms and classes of astrophysical objects have been proposed in the literature [3,21]. Among the proposed candidates for the origin of the highest energy particles the are: i) neutron stars and other compact object [11]; ii) the sources of gamma-ray bursts [20,28]; iii) large-scale shocks due to merging galaxies [5] or in accretion shocks in clusters of galaxies [12]; iv) the active galactic nuclei [23]; v) the hot-spots of FR II radio galaxies [2,24]; vi) the AGN jets by inductive particle acceleration [4,16].

Considering the hypothesis that UHECRs originates from AGNs, and in particular from the hot-spots of FR II sources via Fermi I acceleration, [18] has shown that 15 FR IIs only are lo-

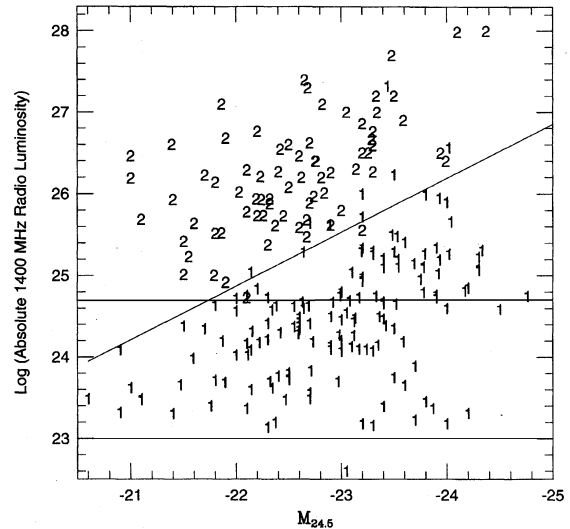


Figure 3. Diagram of a sample of FRI/II objects (from [14]), where the bottom horizontal line (thin solid line) is the limiting power for radio-loud AGN, while the top one (thick solid line) is the limiting power for acceleration of UHECRs with the efficiency  $\eta = 1$  (cf. Eq. 12).

cated within 130 Mpc from us, distance set by the GZK cutoff. Moreover, [15] argues that the FR II sources (NGC4261, PKS1343-60), closest to the highest energy event detected by the Pierre Auger Experiment, were  $\sim 30^\circ$  away from its position. However, more statistics is required before ruling out this possibility.

On the other hand, UHECRs can come from AGN jets themselves, as pointed out by [4,16], by increasing the energy of protons from  $E \leq 10^{18} \text{ eV}$  up to  $E > 10^{19} \text{ eV}$  by electric fields induced in sheared, relativistic magnetized jets, whenever:

$$\vec{\varepsilon} = \nabla\Phi = -\frac{1}{c}\vec{v} \times \vec{B} \rightarrow \Delta\Phi = \frac{1}{c}\vec{B} \cdot (\nabla \times \vec{v}) < 0$$

where  $\vec{\varepsilon}$ ,  $\vec{B}$ ,  $\vec{v}$  are the electric and magnetic fields and jet velocity, respectively, and  $\Phi$  the electric potential. The resulting particle spectrum becomes  $\propto E^{-2}$  asymptotically.

Sheared jets, needed for this kind of acceleration, are actually invoked for interpreting the limb-brightening of radio jets at parsec scales. One must recall that, while FR I jets are non-relativistic at kiloparsec scales and FR II ones are relativistic, VLBI observations of radio galaxies [8] have shown that, albeit these two kind of sources have different radio power and kiloparsec scale morphology, they appear similar at parsec scales where the jet bulk Lorentz factor is typically  $\Gamma = 3 - 10$  for both classes. Moreover, as said before, about ten FR I sources, e.g. M87 [13] and B2 1144+35 [9], observable in the radio band at the VLBI show limb-brightened emission. This limb brightening can be interpreted assuming the presence in the jet of a central spine with high Lorentz factor,  $\Gamma = 5 - 10$ , and an outer layer with  $\Gamma \simeq 2$ . The synchrotron emission from the central spine would be deboosted when viewed at angles larger than about  $30^\circ$ . The problem of the interaction of relativistic, fluid jets with the ambient was studied numerically, in three spatial dimensions, by [25]; they followed the onset and nonlinear growth of unstable modes in the jets while propagating into a uniform medium. The unstable perturbations caused mixing and deceleration of the jet, processes controlled by the initial jet Mach number  $M$  and ambient-to-jet density ratio  $\eta$ , with the jet Lorentz factor kept fixed to 10. They found that very light jets were substantially decelerated, and the jet deceleration was not uniform, but more effective at the outer layers leaving a central “spine” traveling at higher Lorentz factor. Thus, FR I jets as well may meet the conditions to be source of UHECRs via inductive particle acceleration. One can then ask the same question of [18]: how many FR I sources, potential accelerators of cosmic rays, can be found within 100 Mpc from Earth? The radio luminosity function (RLF) of a sample of radio-loud AGNs from the 1.4 GHz NRAO VLA Sky Survey was obtained by [19]. If one extracts from this RLF the number of objects, with luminosity exceeding  $10^{23} \text{ W Hz}^{-1}$ , expected within 100 Mpc from us one finds about 100 sources, that should be identified and their positions possibly correlated to the arrival directions of Pierre Auger events.

### 3.1. A constraint to the jet luminosity

Independently of the particular acceleration mechanism considered, not all radio-loud AGNs can effectively accelerate UHECRs. Cosmic rays must be contained into the acceleration region in order to attain the maximum energies [11], in other words the acceleration timescale must not exceed the dynamical time available for the acceleration. This condition reads, in the frame comoving with the jet:

$$t_{\text{acc}} \leq t_{\text{dyn}} \quad (1)$$

with

$$t_{\text{acc}} = \eta^{-1} t_{\text{L}}, \quad t_{\text{dyn}} = \frac{R}{\beta \Gamma c} \quad (2)$$

where  $\eta \leq 1$  is an efficiency parameter that is appropriate for the actual acceleration mechanism,  $R$  the jet longitudinal coordinate,  $t_{\text{L}} = E/ZeBc$  is the Larmor time in the jet magnetic field,  $\Gamma$  the jet Lorentz factor and  $\beta c$  its velocity. Applying condition (1), one derives the maximum energy achievable, in the observer’s frame [15]:

$$E_{\text{obs}} \leq \eta Z e B R \beta^{-1} \quad (3)$$

This quantity must be related with the jet magnetic field intensity. To the jet total power contribute both kinetic and magnetic (Poynting) luminosities:

$$L_{\text{tot}} = L_{\text{kin}} + L_{\text{B}} \quad (4)$$

with

$$L_{\text{kin}} = 2\pi R^2 \theta^2 (n_0 m c^2) \Gamma (\Gamma - 1) \beta c \quad (5)$$

and

$$L_{\text{B}} = 2\pi R^2 \theta^2 \frac{B^2}{8\pi} \Gamma^2 \beta c \quad (6)$$

where  $\theta$  is the jet opening angle and  $n_0$  the jet density in the comoving frame. Since magnetic fields are likely to play a crucial role in the acceleration process, one may think that the main constituent of jets, close to its origin, is not mass but fields in form of Poynting-dominated beams. However, [26] argued that, even though jets could be Poynting-dominated at the origin,

observational data imply that they become kinetically dominated beyond about 1,000 gravitational radii from the central acceleration region, with at its center a supermassive black-hole of  $\sim 10^8\text{--}10^{10} M_\odot$ . Furthermore, [7] discussed the role of kink instability in Poynting-flux dominated jets and find that the Poynting flux dissipates and the jet becomes kinetically-dominated, again at about 1,000 gravitational radii. Thus it is therefore reasonable to assume that if close to the AGN  $L_{\text{tot}} \approx L_B$ , at the kiloparsec scale  $L_{\text{tot}} \approx L_{\text{kin}}$ .

Combining Eq. 3 with Eq. 6, one obtains [15]:

$$L_B \geq \frac{1}{4}(\eta Z e)^{-2} \theta^2 \Gamma^2 \beta^3 c E_{\text{obs}}^2 \quad (7)$$

As discussed previously, the jet magnetic power is not directly observable, however this form of energy, probably dominant at the beginning, transforms into kinetic one via propagation-related processes. Most importantly, jet kinetic power has been connected to the (observable) luminosity of the radio core by [1] and [10] who derived this quantity from the work done by the radio lobes to evacuate intracluster cavities, seen at the X-ray energy band. They showed a correlation between the kinetic luminosity and the luminosity of the radio core, in the limit of flat power-law spectra of the radio emission ( $\alpha = 0$ ):

$$L_{\text{kin}} = L_{\text{k0}} \left( \frac{L_\nu^{\text{core}}}{L_{\nu 0}} \right)^{12/17} \quad (8)$$

With  $L_{\nu 0} = 7 \times 10^{22} \text{ W Hz}^{-1}$  and  $L_{\text{k0}} = 10^{37} \text{ W}$ . This correlation is shown in the log-log plot of Fig. 4, where the core radio power  $L_R = \nu L_\nu^{\text{core}}$ , with  $\nu = 5 \text{ GHz}$ , and the luminosities are in cgs units.

We have now all the elements for relating condition (7) with quantities *that can be actually observed*. In fact, recalling the above discussion about the transformation of a Poynting-flux dominated jet into a kinetically dominated one, from Eq. (7) and Eq. (8) we derive:

$$L_{\text{k0}} \left( \frac{L_\nu^{\text{core}}}{L_{\nu 0}} \right)^{12/17} \geq \frac{1}{4}(\eta Z e)^{-2} \theta^2 \Gamma^2 \beta^3 c E_{\text{obs}}^2 \quad (9)$$

Solving for  $L_\nu^{\text{core}}$ , and in case of cosmic rays of  $E = 10^{20} \text{ eV}$ , we have:

$$L_\nu^{\text{core}} \geq 10^{24} \left( \eta^{-1} Z^{-1} \theta \Gamma \beta^{3/2} E_{20} \right)^{17/6} \text{ W Hz}^{-1} \quad (10)$$

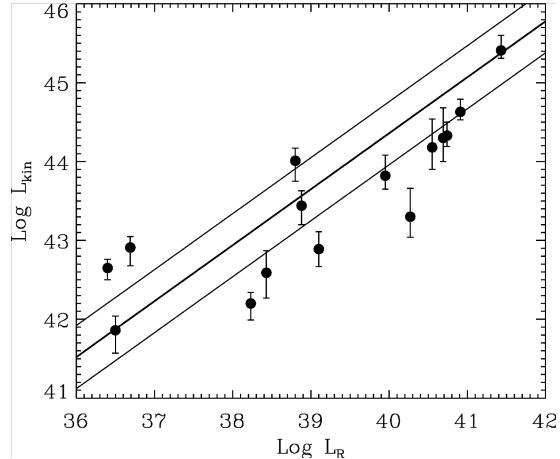


Figure 4. Plot of the kinetic power against the core radio power at 5 GHz (from [10]).

This limit can be checked against observation of  $L_\nu^{\text{core}}$ . However, it can be more instructive to gain a visual impression of this limit, for FR Is, by using Fig. 3. For doing this we must convert the radio core luminosity into the total luminosity. As shown by [8], this two quantities are correlated, once corrected for Doppler effects on the radio flux. Following [8], we set a mean value of  $\Gamma = 5$  for this correction, obtaining:

$$\log L_\nu^{\text{core}} = 0.62 \log L_\nu^{\text{tot}} + 8.41 \quad (11)$$

We may set for the jet velocity  $\beta = 1$ ,  $Z = 1$  for protons, and a typical opening angle of radio jet is  $\theta \approx 10^\circ$ . One thus obtains:

$$L_\nu^{\text{tot}} \geq 7 \times 10^{24} \left( \eta^{-1} \theta_{10} \Gamma_5 E_{20} \right)^{4.6} \text{ W Hz}^{-1} \quad (12)$$

that should be compared with the data in Fig. 3, after having decided which is the favored particle acceleration mechanisms in order to set the parameter  $\eta$ . Setting  $\eta = 1$ , condition (12) is represented in Fig. 3 by the thick, horizontal line. We notice that  $\eta$  cannot attain values much smaller than unity, otherwise we run out of FR I sources suitable for particle acceleration.

We will be then able to look among the about 100 radio-loud AGNs within 100 Mpc the ones

that fulfill condition (12) for accelerating particles up to  $E = 10^{20}$  eV.

#### 4. SUMMARY

We have reviewed the main properties of AGNs, their separation into radio-loud and radio-quiet sources and the implications of this classification on the problem of cosmic ray acceleration from these objects. We have then examined, on quite general bases, the conditions for UHECRs production and set observational limits to the radio luminosity of radio sources in order to be able to be sources of UHECRs.

#### REFERENCES

1. S. W. Allen, R. J. H. Dunn, A. C. Fabian, G. B. Taylor and C. S. Reynolds, *MNRAS* 372 (2006), 21.
2. P. L. Biermann and P. A. Strittmatter, *Ap. J.* 322 (1987) 643.
3. P. L. Biermann, *J. Phys. G: Nucl. Part. Phys.* 23 (1997) 1.
4. R. D. Blandford, *PhST* 85 (2000), 191.
5. C. Cesarsky and V. Ptuskin, 23rd IRCR (University of Calgary) 2 (1993) 341.
6. B. L. Fanaroff and J. M. Riley, *MNRAS* 167 (1974) 31.
7. D. Giannios and H. C. Spruit, *A&A* 450 (2006), 887.
8. G. Giovannini, W. D. Cotton, L. Feretti, L. Lara and T. Venturi, *Ap. J.* 552 (2001), 508.
9. G. Giovannini, M. Giroletti and G.B. Taylor, *A&A* 474 (2007), 409.
10. S. Heinz, A. Merloni and J. Schwab, *Ap. J.* 658 (2007), L9.
11. A. M. Hillas, *Ann. Rev. A&A* 22 (1984) 425.
12. H. Kang, D. Ryu and T. W. Jones, *Ap. J.* 456 (1996) 422.
13. Y. Y. Kovalev, M. L. Lister, D. C. Homan and K. I. Kellermann, *Ap. J.* 668 (2007), 27.
14. M. J. Ledlow and F. N. Owen, *AJ* 112 (1996) 9.
15. M. Lemoine, SF2A-2008: Proceedings of the French Society of Astronomy and Astrophysics Eds.: C. Charbonnel, F. Combes and R. Samadi (<http://proc.sf2a.asso.fr>, p.247).
16. M. Lyutikov and R. Ouyed, *Aph* 27 (2007), 473.
17. S. Massaglia, *Ap&SS* 287 (2003) 223.
18. S. Massaglia, *NuPhS* 165 (2007), 130.
19. T. Mauch and E. M. Sadler, *MNRAS* 375 (2007), 931.
20. M. Milgrom and V. Usov, *Ap. J. Lett.* 449 (1995) L37.
21. M. Nagano and A.A. Watson, *Rev. Mod. Phys.* 72 No. 3 (2000) 689.
22. M. A. Prieto, J. Reunanen, Th. Beckert, K. Tristram, N. Neumayer, J. A. Fernandez and J. Acosta, *ASPC* 373 (2007), 600.
23. R. J. Protheroe and A. P. Szabo, *Phys. Rev. Lett.* 69 (1992) 2885.
24. J. P. Rachen and P. L. Biermann, *A&A* 272 (1993) 161.
25. P. Rossi, A. Mignone, G. Bodo, S. Massaglia, A. Ferrari, *A&A* 488 (2008), 795.
26. M. Sikora, M. C. Begelman, G. M. Madejski and J. -P. Lasota, *Ap. J.* 625 (2005), 72.
27. C. M. Urry and P. Padovani, *PASP* 107 (1995), 803.
28. M. Vietri, *Ap. J.* 453 (1995) 883.